Hindawi Publishing Corporation
Advances in Condensed Matter Physics
Volume 2009, Article ID 361080, 6 pages
doi:10.1155/2009/361080

Research Article

AC Conductivity and Impedance Properties of $0.65Pb(Mg_{1/3}Nb_{2/3})O_3$-$0.35PbTiO_3$ Ceramics

Banarji Behera,[1] E. B. Araújo,[1] R. N. Reis,[1] and J. D. S. Guerra[2]

[1] *Departamento de Física e Química, Universidade Estadual Paulista (UNESP), Caixa Postal 31, 15385-000 Ilha Solteira, SP, Brazil*
[2] *Grupo de Ferroelétricos e Materiais Multifuncionais, Instituto de Física, Universidade Federal de Uberlândia, 38400-902 Uberlâandia, MG, Brazil*

Correspondence should be addressed to Banarji Behera, banarji@dfq.feis.unesp.br

Received 23 October 2008; Revised 14 April 2009; Accepted 2 June 2009

Recommended by R. N. P. Choudhary

The electrical properties of $0.65Pb(Mg_{1/3}Nb_{2/3})O_3$-$0.35(PbTiO_3)$ ceramics over a wide range of frequencies (10^2–10^6 Hz) and temperatures (30–225°C) were studied using impedance spectroscopy technique. The impedance and electric permittivity were strongly temperature and frequency dependent. The activation energy, calculated from the temperature dependence of AC conductivity of the ceramics was found to be ∼0.5 eV. The relaxation process in the ceramics was found to be of non-Debye type. The nature of Cole-Cole diagram reveals the contribution of grain (bulk) and grain boundary permittivity in the ceramics.

1. Introduction

In the recent years lead perovskite relaxor systems such as $Pb(Zn_{1/3}Nb_{2/3})O_3$ (PZN) and $Pb(Mg_{1/3}Nb_{2/3})O_3$ (PMN) have attracted considerable attention due to their exceptionally large dielectric constants and piezoelectric properties [1, 2]. These are characterized by site and charge disorder [3]. They show no symmetry breaking transition on cooling but exhibit strong and frequency dependent peaks in dielectric constants [4, 5]. The disorderness of PMN is reduced by adding $PbTiO_3$ (PT) to PMN [6]. For $x > 0.05$, at low temperature, the $(1 - x)Pb(Mg_{1/3}Nb_{2/3})O_3$-$xPbTiO_3$ (PMN-xPT) is ferroelectric and rhombohedral up to a specific value of x [6]. At higher PT concentration, it undergoes a morphotropic phase transition (at $0.30 < x < 0.40$) [7–9] and becomes tetragonal. At higher temperature, the system becomes paraelectric and cubic for all the value of x. High value of piezoelectric response has been achieved near this transition. For sufficiently high concentrations, the PMN-PT system exhibits ferroelectric tetragonal, rhombohedral, monoclinic, and orthorhombic at low and paraelectric cubic phases at high temperatures [1, 9]. The phase transition between the rhombohedral and tetragonal ferroelectric phases observed by many authors [3, 7, 8, 10]. The PMN-xPT system around the morphotropic phase boundary (MPB) is of special significance for technological applications [11] since the electromechanical response [12] is found to be maximum. Among other MPB systems like $Pb(Zr_xTi_{1-x})O_3$ (PZT) and $(1 - x)Pb(Zr_{1/3}Nb_{2/3})O_3$-$PbTiO_3$ (PZN-xPT), the PMN-xPT is more attractive because it can easily be prepared both in ceramics as well as single crystals. Size driven relaxation and polar states of morphotropic PMN-35PT have been studied by Carreaud et al. using ball mill method [13]. They showed that the dielectric relaxation observed in the range of size 30 nm to ≈200 nm. Further, the dielectric relaxation vanished below the size of ≈30 nm. The processing of $(1 - x)$PMN-xPT ($x = 0.2$, 0.3, 0.35, and 0.4) ceramics from powders synthesized by mechanochemical activation of precursors has been studied by Algueró et al. [14]. They studied these ceramics with a range of grain sizes between 0.2 and 5 μm by varying the PbO partial pressure and temperature. Recently, size effects in MPB of PMN-35PT have also been studied by Algueró et al. [15]. They showed that the decrease of grain size (micron range to approached nanoscale) slows down the transition from the relaxor to the ferroelectric state. All the data reported in the literature are obtained using the fixed frequency measurements. There is enormous literature with different motivations that have

been reported for PMN-PT ceramics or single crystals; it is not purposed to review this literature here. However, there are rare reports on the AC impedance spectroscopy properties of this ferroelectric ceramics with wide frequency range. James et al. [16, 17] reported investigations on relaxor PMN-PT ceramics (x = 0.10) prepared by columbite method. Kobor et al. [18] studied the oxygen vacancies effect on ionic conductivity and relaxation phenomenon in undoped and Mn doped PZN-0.45PT single crystals using impedance spectroscopic in the high temperature region. To the best of our knowledge, no one is reported on the temperature dependence of AC conductivity and impedance properties for PMN-35PT ceramics. In view of what mentioned above, we have reported the impedance spectroscopy studies of $0.65Pb(Mg_{1/3}Nb_{2/3})O_3$-$0.35PbTiO_3$ (PMN-35PT) ceramics to better understand the conduction mechanism of this important ferroelectric composition.

2. Experimental

The complete balanced chemical equation of PMN-35PT is: $0.65Pb(Mg_{1/3}Nb_{2/3})O_3 + 0.35PbTiO_3 = 0.65PMN\text{-}0.35PT$. The ingredients were taken in the desired stoichiometry. The PMN-35PT ceramics studied in the present work was prepared by using columbite method and fine powders obtained from an aqueous solution of oxalic acid (OA) (0.18 mol^{-1}). Then the $MgNb_2O_6$ ($MgO + Nb_2O_5 \rightarrow MgNb_2O_6$) (MN) and the $PbTiO_3$ ($PbO + TiO_2$) (PT) powders were added to this OA solution. The preparation of MN and PT is given in detail elsewhere [19]. The PT–MN–OA was stirred by an ultrasound for 30 minutes. A solution of $Pb(NO_3)_2$ slowly dropped into the PT–MN–OA, resulting in a white precipitate of lead oxalate on the particles of PT and MN. Then the collected mixture was filtered, dried, and ground. After that, an amount of 0.2 g was calcined between 700 and 950°C using an alumina boats. The calcined powder was then cold pressed in to rectangle-sized pellets using a hydraulic pressure. Then the pellets were sintered at 1250°C for 4 hours. The density of the final ceramics was found to be 7.4 gm/cm^3.

In order to study the dielectric and electrical properties of the ceramics, both the flat surfaces of the pellets were polished, and then electroded with air-drying conducting silver paint. After electroding, the pellets were dried at 150°C for 4 hours to remove moisture, if any, and then cooled to room temperature before taking electrical measurements. Dielectric and impedance measurements were carried out using a computer controlled LCR Meter (Agilent; Model 4284A) in a wide frequency (10^2–10^6 Hz) and temperature (28–225°C) range.

The structure of the ceramics was investigated by an X-ray diffraction (XRD) technique at room temperature using Bragg-Brentano geometry in continuous mode with a scanning rate of 1°/minute and step size of 0.02°. The Rigaku Ultima IV diffractometer (operated at 40 kV and 25 mA) with CuK_α radiation (λ = 1.5405 Å) was used. For Rietveld analysis [20], XRD data were input into the GSAS [21] structure refinement code under the EXPGUI [22] interface. Peak profiles were fitted using the Thompson et al. [23] pseudo-Voigt function while a sixth-order polynomial was used to fit the background. The microstructure of the ceramics was observed at room temperature by Scanning Electron Microscope (SEM) (Model Zeiss DSM960).

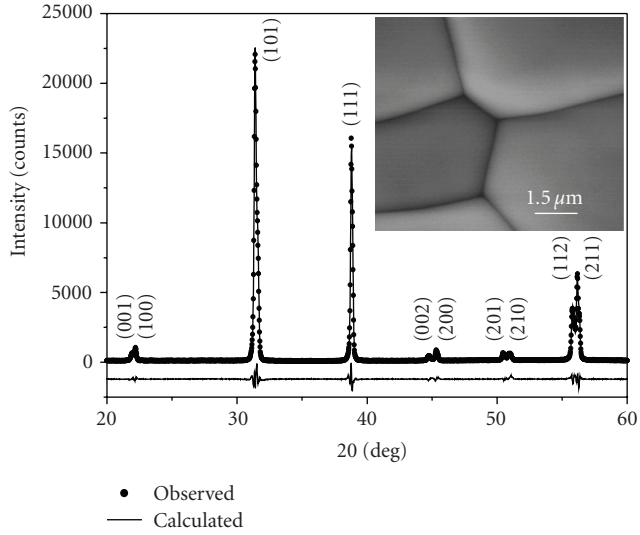

Figure 1: Observed (dots), calculated (continuous line), and difference (bottom line) XRD profiles of PMN-35PT ceramics. Rietveld refinement was performed considering the monoclinic (Pm) and tetragonal (P4mm) phase coexistence model. SEM micrograph of the same ceramics is shown in inset.

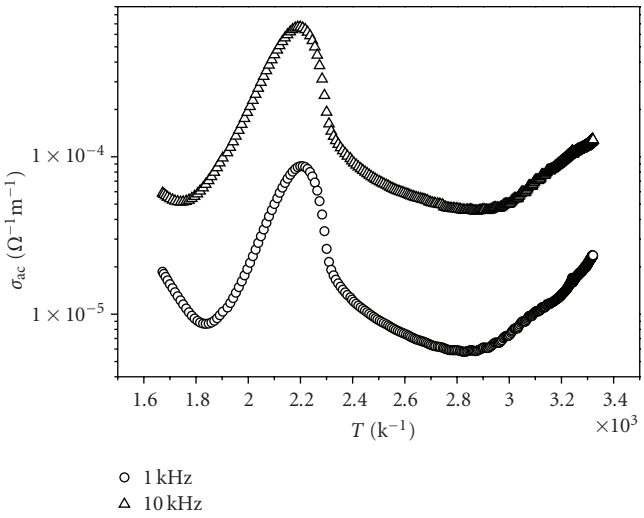

Figure 2: Variation of AC conductivity with 10^3/T at 1 and 10 kHz of PMN-35PT. Measurement performed during cooling.

3. Results and Discussion

3.1. Structural and Microstructural Properties. Rietveld refinements were performed by using the following five different plausible structural models: (i) Rhombohedral phase (R) (R3m space group), (ii) Tetragonal phase (T)

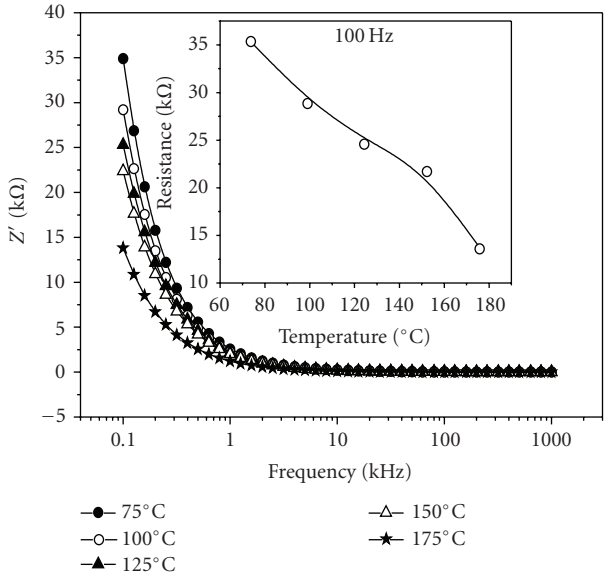

Figure 3: Variation of Z' with frequency at different temperatures of PMN-35PT. Variation of resistance with temperature (inset).

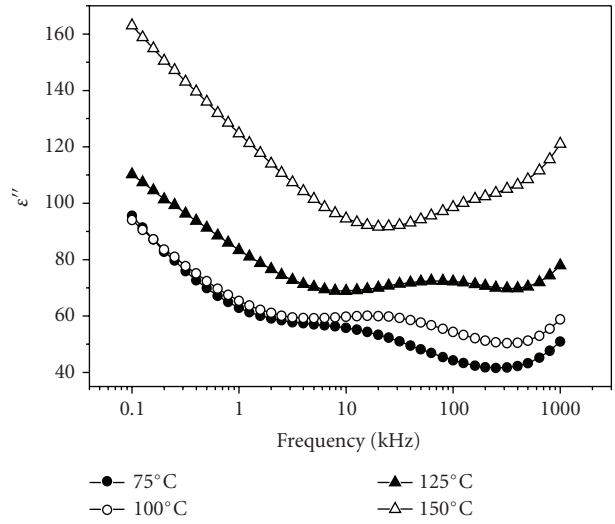

Figure 4: Variation of imaginary ε'' of PMN-35PT with frequency at different temperatures.

(P4mm space group), (iii) Monoclinic phase (M) (Pm space group), (iv) Monoclinic and Tetragonal phase coexistence (M+T), and (v) Tetragonal and Rhombohedral phase coexistence (T+R). These models were used for Rietveld refinements by considering the existence of the monoclinic phase at PMN-PT compositions around the MPB [24]. The main criteria for judging the quality of the fitting are the final fit of the calculated pattern compared with the observed data. However, the R-factors weighted profile R_{wp}, the statistically expected R_{exp}, and the goodness-of-fit indices $\chi^2 = R_{wp}/R_{exp}$ are usually used to attest the quality of a fit [25]. A very good fit was obtained by using the M+T phase coexistence model, leading to the smallest χ^2 (= 2.89) value. This result indirectly attests the good stoichiometry control of the studied ceramics at x = 0.35 mol% of $PbTiO_3$.

Figure 1 shows the observed, calculated, and difference XRD profiles obtained after the Rietveld refinements of the PMN-35PT ceramics, considering the M+T phase coexistence model. Neither pyrochlore phase nor residual phases were observed in this figure. Table 1 summarizes the structural parameters obtained from the Rietveld refinement (shown in Figure 1). A small difference between the observed and calculated profiles attests the good fitting. In addition, a small value obtained for the goodness-of-fit ($\chi^2 = 2.89$) indicates a good refinement. Results obtained in Table 1 confirm that the dominant phase of PMN-35PT presents a tetragonal structure of 67 mol% compared with monoclinic structure of 33 mol%. In other words, the minority monoclinic phase coexists with the tetragonal phase in the PMN-35PT ceramics. These results are in good agreement with the reported one for the same PMN-35PT composition [24]. Figure 1 (inset) shows the scanning electron micrograph (SEM) of the PMN-35PT ceramics using fractured samples. In this micrograph no secondary phases are observed between grains. The grains are densely distributed over the surface of the sample without porosity. The average grain size was estimated to be 7.8 μm.

3.2. AC Conductivity Studies. Figure 2 shows the AC conductivity (σ_{ac}) with 10^3/T at 1 and 10 kHz for PMN-35PT ceramics. A maximum is observed in ac conductivity at around 454 K for both frequencies, which is closely related to the ferroelectric-paraelectric phase transition (T_c). This is the normal behavior of a ferroelectric material. This behavior can be attributed to the relaxation process associated with the domain reorientation, domain wall motion, and the dipolar behavior [3]. There are distinct region of conduction mechanisms in different temperature ranges: (i) n and/or p-type hopping charge (corresponding to low temperatures), (ii) small polarons and oxygen vacancy conduction (at intermediate temperature regions), and (iii) intrinsic ionic conduction (at high temperature region) [26]. The nature of variation of σ_{ac} over a wide temperature range supports the thermally activated transport properties of the ceramics obeying Arrhenius equation $\sigma = \sigma_0 \exp(-E_a/kT)$ (where σ_0 = pre-exponential factor, k = Boltzmann's constant). The value of activation energy (E_a) of the ceramics at 1 and 10 kHz was found to be 0.46 and 0.21 eV (275–325°C, i.e., in the $T \geq T_c$) and 0.20 and 0.19 eV (100–150°C, i.e., in the $T \leq T_c$), which is quite consistent with that of other complex perovskites [27, 28]. The value obtained below the transition temperature ($T \geq T_c$) is in good agreement with those of 67PMN-33PT single crystals [29]. The activation energy was found to decrease on increasing frequency. This behavior suggests that the conduction mechanism may be due to the hopping of charge carriers (i.e., n and/or p-type) from one site to the other. Therefore, very small amount of energy is required to activate the charge carriers/electrons for electrical conduction. It has been shown by Ang et al. [30] and Moretti and Michel-Calendini [31] that the value of activation energy depends on ionization level of the oxygen vacancy. Usually, activation energy less than 1.0 eV is

Table 1: Refined structural parameters of PMN-35PT ceramics using the coexistence model between tetragonal phase (space group P4mm) and monoclinic phase (space group Pm).

	Tetragonal phase (space group P4mm) $a = b = 3.997(4)$ Å, $c = 4.046(1)$ Å, $\alpha = \beta = \gamma = 90^\circ$, $R_{wp} = 9.40\%$, $R_{exp} = 5.53\%$ e $\chi^2 = 2.89$				Monoclinic phase (space group Pm) $a = 4.026(9)$ Å, $b = 4.001(6)$, $c = 4.052(9)$ Å, $\alpha = \gamma = 90^\circ$, and $\beta = 90, 60(2)^\circ$			
	x_T	y_T	z_T	U (Å^2)	x_M	y_M	z_M	U (Å^2)
	0.000	0.000	—	$U_{11} = 31.59(2)$	0.028(1)	0.000	0.025(3)	$U_{11} = 80.0(7)$
Pb^{2+}	—	—	0.003(2)	$U_{22} = 31.59$	—	—	—	$U_{22} = 79.96$
	—	—	—	$U_{33} = 31.59$	—	—	—	$U_{33} = 79.96$
Ti^{4+}/	0.500	0.500	0.571(8)	Uiso = 9.0(1)	0.490(5)	0.500	0.539(1)	Uiso = 45.0(5)
Nb^{5+}	0.500	0,500	0,418(1)	Uiso = 68,7(4)	0,488(5)	0,500	0,542(9)	Uiso = 46,9(21)
Mg^{2+}	0,500	0.500	0.570(1)	Uiso = 9.0(25)	0.493(6)	0.500	0.537(1)	Uiso = 39.0(13)
O_I^{2-}	0.500	0.500	0.156(5)	Uiso = 8.94(7)	0.496(6)	0.500	0.059(2)	Uiso = 67.0(7)
O_{II}^{2-}	0.500	0.000	0.553(6)	Uiso = 9.0(7)	0.505(5)	0.000	0.565(1)	Uiso = 29.0(4)
Ratio	67 mol% (Tetragonal)				33 mol% (Monoclinic)			

connected to singly ionized vacancies [30] and/or electronic mobility in space charge regions [32]. Thus, the conduction process within this temperature range may be due to the hopping of charge carriers and/or singly ionized oxygen vacancies of the ceramics.

3.3. Impedance Studies. The complex impedance spectroscopic (CIS) technique [33] is used to analyze the electrical response of polycrystalline sample in a wide range of frequencies. Electrical ac data may be represented in any of the four basic formalisms [34] which are interrelated to each other:

$$\begin{aligned}
&\text{Complex impedance} : Z^* = Z' - jZ'',\\
&\text{Complex admittance} : Y^* = (Z^*)^{-1},\\
&\text{Complex permittivity} : \varepsilon^* = [j\omega C_0 Z^*]^{-1} = \varepsilon' - j\varepsilon'',\\
&\text{Complex electric modulus} : M^* = j\omega C_0 Z^* = M' + jM'',
\end{aligned} \tag{1}$$

where (Z', M', ε') and $(Z'', M'', \varepsilon'')$ are the real and imaginary components of impedance, modulus, and permittivity, respectively, $j = \sqrt{-1}$, $\omega\ (= 2\pi f)$ is the angular frequency and $C_0 = \varepsilon_0 A\ell^{-1}$ in which C_0 is the vacuum capacitance of the cell without the sample, ε_0 the permittivity of free space, 8.854×10^{-14} F·cm^{-1}, ℓ and A are the thickness and area of the sample. In the present paper we are basically focus on the complex impedance and complex permittivity part.

Figure 3 shows the behavior of real part of impedance (Z') as a function of frequency at different temperatures (i.e., 75–175°C) of PMN-35PT. It is observed that the magnitude of Z' (bulk resistance) decreases on increasing temperature in the low frequency ranges (up to a certain frequency), and thereafter appears to merge in the high-frequency region. This may possibly be due to the release of space charge polarization with rise in temperatures and frequencies [35]. This behavior shows that the conduction mechanism increases with increasing temperature and frequency (i.e., negative temperature coefficient of behavior like that of a semiconductor). The decreasing behavior of resistance with temperature at 100 Hz is (inset of Figure 3).

Figure 4 shows the imaginary permittivity (ε'') as a function of frequency at different temperatures. The nature of variation of ε'' shows the existence of peak at a particular frequency (f_{max}) at different temperatures. The peak frequency shifts towards the higher side on increasing temperature, and above 150°C, the peak disappears from the frequency range of investigation. The value of ε'' decreases with rise in frequency up to a certain frequency and thereafter increases to a maximum at a higher frequency. This type of nature of variation is very much comparable with the high dielectric constant materials [16, 17]. Though structural, dielectric, and ferroelectric properties of PMN-35PT studied [19], this type of dispersion has not been reported earlier.

In order to carry out the thorough studies of permittivity and their temperature dependence, it is necessary to separate the contribution of grain, grain boundary, and material electrode interface effect. For this, we have taken the real and imaginary parts of permittivity as $\varepsilon' = -Z''/\omega C_0(Z'^2 + Z''^2)$ and $\varepsilon'' = Z'/\omega C_0(Z'^2 + Z''^2)$. Figure 5 shows the complex permittivity (ε^*) spectrum (Cole-Cole plot) for two distinct temperatures (100°C and 125°C). From this figure it is clear that a polydispersive nature of dielectric phenomena in PMN-35PT with the possibility of distributed relaxation time, as indicated by the semicircular arc at different temperatures with their center located below the real x-axis. This indicates that the relaxation process is of non-Debye type. This nature of complex dielectric spectrum is well described by an empirical relation (developed by Cole-Cole), [36] and is expressed by

$$\varepsilon^* = \varepsilon' - i\varepsilon'' = \varepsilon_\infty + \frac{\Delta\varepsilon}{1 + (i\omega\tau)^{1-\alpha}}, \tag{2}$$

where $\Delta\varepsilon = \varepsilon_s - \varepsilon_\infty$ is the dielectric relaxation strength (ε_s and ε_∞ are the static and infinite frequency dielectric

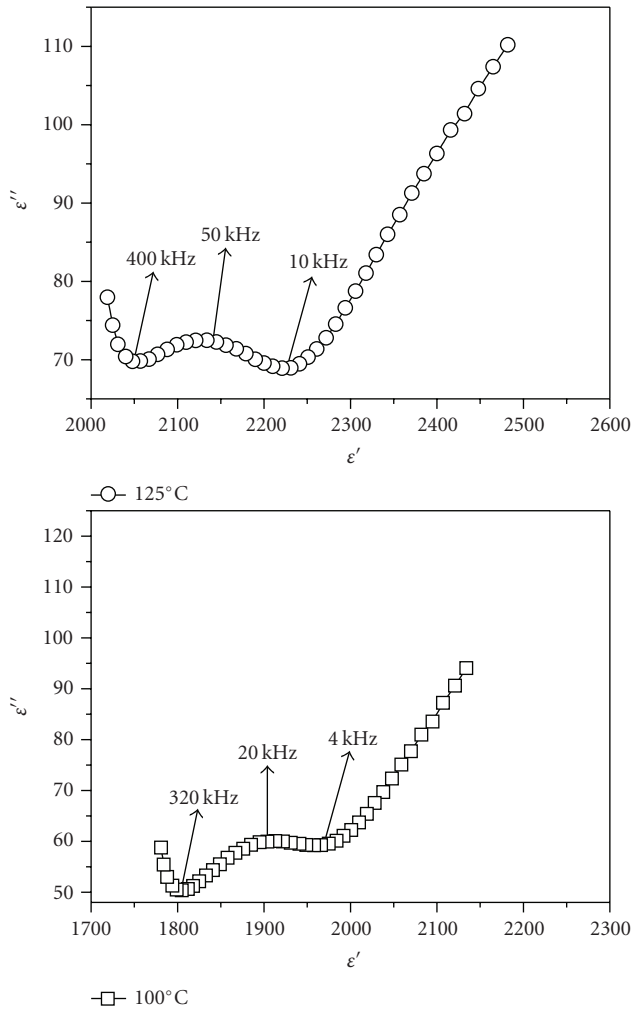

Figure 5: Complex permittivity spectrum (Cole-Cole plot) of PMN-35PT at 100 and 125°C.

constants), τ is relaxation time, and α is a parameter describing the distribution of relaxation time. The value of $\alpha = 0$ describes monodispersive relaxation of Debye type, while $0 \leq \alpha \leq 1$ indicates a nonuniform distribution of relaxation time with asymmetric relaxation peak in the complex impedance spectrum. At low frequency region (up to 4 kHz and 10 kHz at 100°C and 125°C, resp.), the appearance of a spike is observed. This may be attributed to the diffusion phenomena of Warburg type [37], and arising due to charge carrier transport at these temperatures. This may also be associated either with a surface layer ceramics or with electrode polarization process [38]. In the intermediate frequency range, a complete semicircle is observed which may be due to the effect grain boundary permittivity [39]. A trend of formation of a semicircular arc is observed, although there is a lack of experimental data (>1 MHz) to complete the semicircle in the high frequency region (above 320 kHz and 400 kHz at 100°C and 125°C, resp.). This may be assumed due to the contribution of bulk permittivity of the ceramics. The above result indicates intrinsic properties of the materials with loss in polarization processes yielding from the mobility of ions.

4. Conclusions

The electrical properties of PMN-35PT ceramics were studied using impedance spectroscopic technique. The ceramics has relaxation phenomena, which could be attributed to a non-Debye type. The impedance parameters were found to be strongly frequency and temperature dependent. The conduction mechanism in the ceramics may be due to the hopping of charge carriers and/or singly ionized. Cole-Cole plots show the contribution of grain (bulk) and grain boundary permittivity in the ceramics. Using impedance spectroscopic technique, studies of different PMN-xPT compositions around the morphotropic phase boundary are in progress to understand the dielectric relaxation mechanism as well as the electrical properties.

Acknowledgments

The authors would like to express their gratitude to Brazilian agencies FAPESP (Processes: 2007/00183-7 and 2007/05302-4), CNPq (Research Grant: 301382/2006-9) and CAPES for the financial support. Finally, we would like to thank Companhia Brasileira de Metalurgia e Mineração (CBMM) for providing the reagents used in this work.

References

[1] S.-E. Park and T. R. Shrout, "Ultrahigh strain and piezoelectric behavior in relaxor based ferroelectric single crystals," *Journal of Applied Physics*, vol. 82, no. 4, pp. 1804–1811, 1997.

[2] A. A. Bokov and Z.-G. Ye, "Recent progress in relaxor ferroelectrics with perovskite structure," *Journal of Materials Science*, vol. 41, no. 1, pp. 31–52, 2006.

[3] L. E. Cross, "Relaxor ferroelectrics," *Ferroelectrics*, vol. 76, pp. 241–267, 1987.

[4] A. Levstik, Z. Kutnjak, C. Filipič, and R. Pirc, "Glassy freezing in relaxor ferroelectric lead magnesium niobate," *Physical Review B*, vol. 57, no. 18, pp. 11204–11211, 1998.

[5] Z. Kutnjak, C. Filipič, R. Pirc, A. Levstik, R. Farhi, and M. El Marssi, "Slow dynamics and ergodicity breaking in a lanthanum-modified lead zirconate titanate relaxor system," *Physical Review B*, vol. 59, no. 1, pp. 294–301, 1999.

[6] E. V. Colla, N. K. Yushin, and D. Viehland, "Dielectric properties of $(PMN)_{(1-x)}(PT)_x$ single crystals for various electrical and thermal histories," *Journal of Applied Physics*, vol. 83, no. 6, pp. 3298–3304, 1998.

[7] G. Xu, D. Viehland, J. F. Li, P. M. Gehring, and G. Shirane, "Evidence of decoupled lattice distortion and ferroelectric polarization in the relaxor system PMN-*x*PT," *Physical Review B*, vol. 68, no. 21, Article ID 212410, 4 pages, 2003.

[8] F. Bai, N. Wang, J. Li, et al., "X-ray and neutron diffraction investigations of the structural phase transformation sequence under electric field in $0.7Pb(Mg_{1/3}Nb_{2/3})$-$0.3PbTiO_3$ crystal," *Journal of Applied Physics*, vol. 96, no. 3, pp. 1620–1627, 2004.

[9] B. Noheda, "Structure and high-piezoelectricity in lead oxide solid solutions," *Current Opinion in Solid State and Materials Science*, vol. 6, no. 1, pp. 27–34, 2002.

[10] D. Viehland, J. F. Li, S. J. Jang, L. E. Cross, and M. Wuttig, "Glassy polarization behavior of relaxor ferroelectrics," *Physical Review B*, vol. 46, no. 13, pp. 8013–8017, 1992.

[11] K. Uchino and J. R. Giniewicz, *Micromechatronics*, Marcel Dekker, New York, NY, USA, 2003.

[12] B. Jaffe, W. R. Cook, and H. Jaffe, *Piezoelectric Ceramics*, Academic Press, London, UK, 1971.

[13] J. Carreaud, P. Gemeiner, J. M. Kiat, et al., "Size-driven relaxation and polar states in $PbMg_{1/3}Nb_{2/3}O_3$-based system," *Physical Review B*, vol. 72, no. 17, Article ID 174115, 6 pages, 2005.

[14] M. Alguero, A. Moure, L. Pardo, J. Holc, and M. Kosec, "Processing by mechanosynthesis and properties of piezoelectric $Pb(Mg_{1/3}Nb_{2/3})O_3$-$PbTiO_3$ with different compositions," *Acta Materialia*, vol. 54, no. 2, pp. 501–511, 2006.

[15] M. Alguero, J. Ricote, R. Jiménez, et al., "Size effect in morphotropic phase boundary $Pb(Mg_{1/3}Nb_{2/3})$ O_3-$PbTiO_3$," *Applied Physics Letters*, vol. 91, no. 11, Article ID 112905, 2007.

[16] A. R. James and K. Srinivas, "Low temperature fabrication and impedance spectroscopy of PMN-PT ceramics," *Materials Research Bulletin*, vol. 34, no. 8, pp. 1301–1310, 1999.

[17] A. R. James, S. Priya, K. Uchino, and K. Srinivas, "Dielectric spectroscopy of $Pb(Mg_{1/3}Nb_{2/3})O_3$-$PbTiO_3$ single crystals," *Journal of Applied Physics*, vol. 90, no. 7, pp. 3504–3508, 2001.

[18] D. Kobor, B. Guiffard, L. Lebrun, A. Hajjaji, and D. Guyomar, "Oxygen vacancies effect on ionic conductivity and relaxation phenomenon in undoped and Mn doped PZN-4.5PT single crystals," *Journal of Physics D*, vol. 40, no. 9, pp. 2920–2926, 2007.

[19] E. B. Araújo, R. N. Reis, C. A. Guarany, et al., "Synthesis of slightly < 111 >-oriented $0.65Pb(Mg_{1/3}Nb_{2/3})O_3$-$0.35PbTiO_3$ ceramic prepared from fine powders," *Materials Chemistry and Physics*, vol. 104, no. 1, pp. 40–43, 2007.

[20] H. M. Rietveld, "Line profiles of neutron powder-diffraction peaks for structure refinement," *Acta Crystallographica*, vol. 22, pp. 151–152, 1967.

[21] A. C. Larson and R. B. Von Dreele, "General structure analysis system," Tech. Rep. LAUR 86, Los Alamos National Laboratory, 1994.

[22] B. H. Toby, "EXPGUI, a graphical user interface for GSAS," *Journal of Applied Crystallography*, vol. 34, no. 2, pp. 210–213, 2001.

[23] P. Thompson, D. E. Cox, and J. B. Hastings, "Rietveld refinement of Debye-Scherrer synchrotron X-ray data from Al_2O_3," *Journal of Applied Crystallography*, vol. 20, pp. 79–83, 1987.

[24] A. K. Singh and D. Pandey, "Evidence for M_B and M_C phases in the morphotropic phase boundary region of (1-x)$[Pb(Mg_{1/3}Nb_{2/3})O_3]$-$xPbTiO_3$: a rietveld study," *Physical Review B*, vol. 67, no. 6, Article ID 064102, 12 pages, 2003.

[25] L. B. Mccusker, R. B. Von Dreele, D. E. Cox, D. Louër, and P. Scardi, "Rietveld refinement guidelines," *Journal of Applied Crystallography*, vol. 32, no. 1, pp. 36–50, 1999.

[26] O. Raymond, R. Font, N. Suarez-Almodovar, J. Portelles, and J. M. Siqueiros, "Frequency-temperature response of ferroelectromagnetic Pb $(Fe_{1/2}Nb_{1/2})O_3$ ceramics obtained by different precursors—part I. Structural and thermo-electrical characterization," *Journal of Applied Physics*, vol. 97, no. 8, Article ID 084107, 8 pages, 2005.

[27] N. V. Prasad, G. Prasad, T. Bhimasankaram, S. V. Suryanarayana, and G. S. Kumar, "Synthesis, impedance and dielectric properties of $LaBi_5Fe_2Ti_3O_{18}$," *Bulletin of Materials Science*, vol. 24, no. 5, pp. 487–495, 2001.

[28] K. I. Gnanasekar, V. Jayaraman, E. Prabhu, T. Gnanasekaran, and G. Periaswami, "Electrical and sensor properties of $FeNbO_4$: a new sensor material," *Sensors and Actuators B*, vol. 55, no. 2, pp. 170–174, 1999.

[29] F. Kochary, M. D. Aggarwal, A. K. Batra, R. Hawrami, D. Lianos, and A. Burger, "Growth and electrical characterization of the lead magnesium niobate-lead titanate (PMN-PT) single crystals for piezoelectric devices," *Journal of Materials Science: Materials in Electronics*, vol. 19, no. 11, pp. 1058–1063, 2008.

[30] C. Ang, Z. Yu, and L. E. Cross, "Oxygen-vacancy-related low-frequency dielectric relaxation and electrical conduction in $Bi:SrTiO_3$," *Physical Review B*, vol. 62, no. 1, pp. 228–236, 2000.

[31] P. Moretti and F. M. Michel-Calendini, "Impurity energy levels and stability of CR and MN ions in cubic $BaTiO_3$," *Physical Review B*, vol. 36, no. 7, pp. 3522–3527, 1987.

[32] N. Ortega, A. Kumar, R. S. Katiyar, and J. F. Scott, "Maxwell-Wagner space charge effects on the Pb (Zr,Ti) O_3-$CoFe_2O_4$ multilayers," *Applied Physics Letters*, vol. 91, no. 10, Article ID 102902, 2007.

[33] J. R. MacDonald, *Impedance Spectroscopy*, Wiley, New York, NY, USA, 1987.

[34] I. M. Hodge, M. D. Ingram, and A. R. West, "Impedance and modulus spectroscopy of polycrystalline solid electrolytes," *Journal of Electroanalytical Chemistry*, vol. 74, no. 2, pp. 125–143, 1976.

[35] R. N. P. Choudhary, D. K. Pradhan, C. M. Tirado, G. E. Bonilla, and R. S. Katiyar, "Structural, dielectric and impedance properties of $Ca(Fe_{2/3}W_{1/3})O_3$ nanoceramics," *Physica B*, vol. 393, no. 1-2, pp. 24–31, 2007.

[36] K. S. Cole and R. H. Cole, "Dispersion and absorption in dielectrics I. Alternating current characteristics," *The Journal of Chemical Physics*, vol. 9, no. 4, pp. 341–351, 1941.

[37] E. Warburg, "Ueber die eolarisations Capacitat des Platins," *Annals of Physics*, vol. 6, pp. 125–135, 1901.

[38] J. East and D. C. Sinclair, "Characterization of $(Bi_{1/2}Na_{1/2})TiO_3$ using electric modulus spectroscopy," *Journal of Materials Science Letters*, vol. 16, no. 6, pp. 422–425, 1997.

[39] N. Hirose and A. R. West, "Impedance spectroscopy of undoped $BaTiO_3$ ceramics," *Journal of the American Ceramic Society*, vol. 79, no. 6, pp. 1633–1641, 1996.